

# 10

## A Current Based VLSI Degree-Two Chaos Generator

Li Wang<sup>1</sup> Yu Jiang<sup>2</sup> and Robert Newcomb<sup>3</sup>

<sup>1</sup> Department of Computer and Electrical Engineering  
University of Maryland, College Park, Maryland, 20742 USA  
wangli@glue.umd.edu

<sup>2</sup> Department of Computer and Electrical Engineering  
University of Maryland, College Park, Maryland, 20742 USA  
jiangyu@glue.umd.edu

<sup>3</sup> Department of Computer and Electrical Engineering  
University of Maryland, College Park, Maryland, 20742 USA  
newcomb@glue.umd.edu

### Abstract

In this chapter, a current based VLSI degree-two chaos generator is presented. The generator is based upon two unstable oscillators with feedbacks to themselves. The stability of the system is realized via the use of binary hysteresis. The chaotic nature of the signals is guaranteed by the Li-Yorke theorem through the generation of the period-three return map. The initial conditions of the system are discussed and an approach to change them to the origin is proposed. The simulation results are presented finally.

## 10.1 Introduction

Synthesis of simple chaotic oscillators has been studied extensively due to interest in investigating nonlinear phenomena. The idea of using hysteresis for generating chaos was suggested by Rössler [1]. In recent years, a number of hysteresis chaos generators have been published [2], [3], and [4].

This chapter is an extension of former work [2]. The 2-D chaotic signals presented in this chapter are generated in current based instead of voltage mode in [2]. Chaos is generated in this case by creating two planes in which second-order linear but unstable pseudo-trajectories are formed. However, because of hysteresis in the system, the true trajectories jump between these pseudo-trajectories in such a manner that the jump points are eventually fed back inside themselves so that a period-three return map is generated. That period-three implies chaos was proved by Li and Yorke [5].

First three of the following sections serve as a review of mathematical ideas. In Sec. 1.2, we review former research on binary hysteresis chaos generation systems as presented in [2]. The Li and Yorke theorem [5] is explained briefly in Sec. 1.3. In Sec. 1.4, we present a full discussion of binary hysteresis, including the mathematical model used, which is based on former work [6], and the design parameters for hysteresis generation. In Sec. 1.5, the current work on chaos generation through current based VLSI CMOS circuits are presented along with VLSI CMOS synthesis. A discussion on the system initial conditions is given in the Sec. 1.6. In Sec. 1.7, PSPICE simulation results are discussed.

## 10.2 Degree-Two Chaos Generation System

### 10.2.1 System description of degree-two chaos generation using binary hysteresis

In this section, we outline the main ideas to give a physical insight into how the binary hysteresis chaos generation system works. Figure 10.1 shows a three-dimensional view of the system operation. There are two half planes in the three-dimensional space, an upper plane and a lower plane. On each of the planes the trajectories are continuous until they meet the edges and jump to the other plane. For instance, we can trace the trajectory from point *a*. When it hits the edge of the lower half plane, it jumps from point 4 to point 5 in the upper plane. If we look down on the space from above, all trajectories are smooth and continuous except boundary points, which indicates that the system jumps from one state to the other.

The points on the trajectories, which are in fact spirals, are actually points on the true continuous-time trajectories. By controlling the spiral parameters, the placement of the spiral centers and their shapes are able to be controlled,

FIGURE 10.1  
3-D view of che

thereby enablir

If we plot th  
of previous cro  
map. By adjusti  
chaotic propert  
of the system (  
has a point of  
turn to point *c*,  
made equal to

### 10.2.2 Semi

In this section  
system. We b  
electronic reali:

extensively due to in-  
of using hysteresis for  
ent years, a number of  
and [4].  
he 2-D chaotic signals  
nstead of voltage mode  
planes in which second-  
ed. However, because  
between these pseudo-  
eventually fed back inside  
ted. That period-three

of mathematical ideas.  
erisis chaos generation  
] is explained briefly in  
ry hysteresis, including  
ork [6], and the design  
current work on chaos  
s are presented along  
m initial conditions is  
results are discussed.

generation using

al insight into how the  
re 10.1 shows a three-  
two half planes in the  
plane. On each of the  
he edges and jump to  
y from point a. When  
point 4 to point 5 in  
above, all trajectories  
ich indicates that the

ls, are actually points  
the spiral parameters,  
able to be controlled,

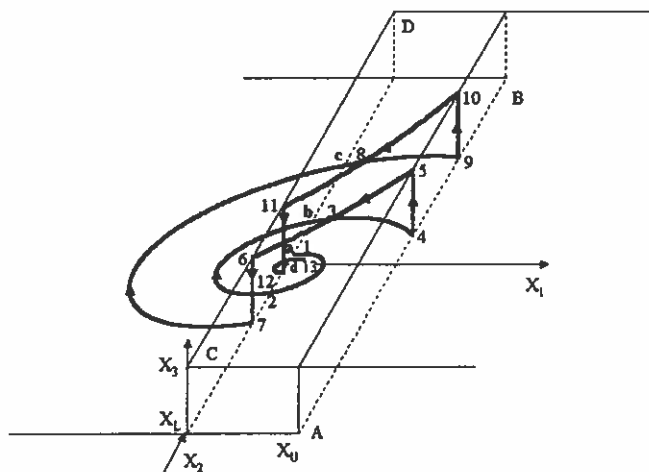


FIGURE 10.1  
3-D view of chaos system [2].

thereby enabling us to make the system have chaotic properties [2].

If we plot the points of return to the upper half  $x_2$  axis versus the points of previous crossing with upper  $x_2$  axis, we obtain an upper half axis return map. By adjusting the system parameters, we are able to make the system have chaotic properties. The theorem of Li and Yorke shows that the trajectories of the system ( $x_2$  versus time) are chaotic if the return map is continuous and has a point of period three. In Fig. 10.1, point a leads to point b and that in turn to point c, and finally to point d, which will be a period three point if it is made equal to a. We will discuss this in more detail in the following sections.

10.2.2 Semistate equations and solutions

In this section we will develop the system equations for our chaos generation system. We begin with semistate type equations in a form suitable for the electronic realization:

$$\begin{aligned} \frac{dX_1}{dt} &= \omega_0 X_2 + a_1 \omega_0 H(X_3), \\ \frac{dX_2}{dt} &= -\omega_0 X_1 - 2\sigma \omega_0 X_2 + a_2 \omega_0 H(X_3), \\ X_3 &= b_1 X_1 + b_2 X_2. \end{aligned} \tag{10.2.1}$$

Here  $H(\cdot)$  is a binary hysteresis function, which is of the form (refer to Eq. (10.4.26) also):

$$H(X_3) = \begin{cases} H_+ & \text{if } X_L < X_3, \\ H_- & \text{if } X_3 < X_U, \end{cases} \quad (10.2.2)$$

$\sigma, a_1, a_2, b_1, b_2$  and  $\omega_0$  are system design parameters.

Because of the existence of a binary hysteresis function, the system equations have two states. The equilibrium points (when the time derivative of  $X_1$  and  $X_2$  are zero) are:

Lower plane:

$$[X_1, X_2] = [(2\sigma a_1 + a_2)H_-, -a_1H_-]. \quad (10.2.3)$$

Upper plane:

$$[X_1, X_2] = [(2\sigma a_1 + a_2)H_+, -a_1H_+]. \quad (10.2.4)$$

From the equation we see that we can move these equilibrium points independently via system parameters. For simplicity we choose the hysteresis dependent on  $X_1$  only and let  $\omega_0$  be 1, i.e.:

$$\begin{aligned} b_1 &= 1, & b_2 &= 0, \\ \omega_0 &= 1. \end{aligned} \quad (10.2.5)$$

We transform the equilibrium point on the lower plane to the origin via moving coordinates, and simplify cofactors of equations by scaling:

$$\begin{aligned} x_1 &= \frac{X_1 - (2\sigma a_1 + a_2)H_-}{H_+ - H_-}, \\ x_2 &= \frac{X_2 + a_1H_-}{H_+ - H_-}. \end{aligned} \quad (10.2.6)$$

Finally, by substituting Eqs. (10.2.5) to (10.2.6) into Eq. (10.2.1), we obtain a normalized set of equations:

$$\begin{aligned} \frac{dx_1}{dt} &= x_2 + a_1h(x_1), \\ \frac{dx_2}{dt} &= -x_1 - 2\sigma x_2 + a_2h(x_1), \end{aligned} \quad (10.2.7)$$

where the normalized hysteresis is of the form

$$h(x) = \begin{cases} 1 & \text{if } x_l \leq x, \\ 0 & \text{if } x \geq x_u. \end{cases} \quad (10.2.8)$$

The equilibrium points of the normalized equations are then:

Lower plane:

Upper plane:

Thus we see that the relative locations of the

which actually puts the

The two spirals repres  
Therefore the design pa  
lower spiral. We pick  $\sigma$   
of the upper half-axis re  
We will discuss this in 1

Here we conveniently  
of chaos generated.

The solution for Eq.  
 $x(t)$   
 $y(t)$

where  
 $\omega = (1 - \sigma)$   
 $\angle s = \arctan$

This is the spiral of the  
for the upper plane spir

$$\begin{aligned} x(t) &= K(e \\ y(t) &= K(e \end{aligned}$$

Both  $K$  and the angle  $\phi$   
[ $X, Y$ ] on the trajectory  
if  $X \neq 0$ :

$$\begin{aligned} K &= [\text{sign } X][X^2 + \\ \phi &= \arcsin[(Y + \sigma] \end{aligned}$$

form (refer to Eq. (10.4.26)

(10.2.2)

Lower plane:

$$[x_1, x_2] = [0, 0]. \tag{10.2.9}$$

Upper plane:

$$[x_1, x_2] = [2\sigma a_1 + a_2, -a_1]. \tag{10.2.10}$$

Thus we see that the ratio of  $\sigma a_1$  to  $a_2$  is the design parameter deciding the relative locations of the two spirals. For convenience we choose

$$a_1 = -1, \tag{10.2.11}$$

which actually puts the center of the upper plane spiral on the line  $x_2 = 1$ .

The two spirals represented by Eq. (10.2.7) are actually identical in the shape. Therefore the design parameter  $\sigma$  controls the shape for both upper spiral and lower spiral. We pick  $\sigma$  as a convenient number with  $a_2$  to ensure the continuity of the upper half-axis return map, a necessary condition for chaotic properties. We will discuss this in more detail in the next section.

Here we conveniently choose  $x_l = 0$ .  $x_u$  is designed to adjust the amplitude of chaos generated.

The solution for Eq. (10.2.7), the spiral in the lower plane, is:

$$x(t) = K(\exp[-\sigma t]) \cos[\omega t + \phi], \tag{10.2.12}$$

$$y(t) = K(\exp[-\sigma t]) \cos[\omega t + \phi + \angle s],$$

where

$$\omega = (1 - \sigma^2)^{1/2}, \tag{10.2.13}$$

$$\angle s = \arctan[\omega/(-\sigma)] = \text{angle of } (-\sigma + j\omega).$$

This is the spiral of the lower plane, with its center at the origin. The results for the upper plane spiral are of the form:

$$x(t) = K(\exp[-\sigma t]) \cos[\omega t + \phi] - 2\sigma a_1 - a_2, \tag{10.2.14}$$

$$y(t) = K(\exp[-\sigma t]) \cos[\omega t + \phi + \angle s] + a_1.$$

Both  $K$  and the angle  $\phi$  are constant, and can be decided from any given point  $[X, Y]$  on the trajectory.

if  $X \neq 0$ :

$$K = [\text{sign } X][X^2 + 2\sigma XY + Y^2]^{1/2}/\omega, \tag{10.2.15}$$

$$\phi = \arcsin[(Y + \sigma X)/(-\omega K)] = \arctan[(Y + \sigma X)/(-\omega X)].$$

on, the system equations  
ne derivative of  $X_1$  and

(10.2.3)

(10.2.4)

ilibrium points indepen-  
se the hysteresis depen-

(10.2.5)

plane to the origin via  
is by scaling:

(10.2.6)

Eq. (10.2.1), we obtain a

(10.2.7)

(10.2.8)

re then:

if  $X = 0$ :

$$K = -Y/\omega, \tag{10.2.16}$$

$$\phi = \pi/2.$$

Every time the trajectory jumps from one plane to the other, the parameters  $K$  and  $\phi$  need to be recalculated. With all the information above, and knowing the parameters  $x_u, a_2$  and  $\sigma$ , we are now able to calculate the trajectories using a computer.

### 10.3 Chaotic Nature of the System

#### 10.3.1 The Li-Yorke theorem

In this section we will give a statement of the theorem first [5], then we will show how the system satisfies the conditions for chaos.

This theorem considers iterates of continuous maps  $M$ . The maps are defined by

$$x = M_0(x), \tag{10.3.17}$$

$$M_n(x) = M_{n-1}(M(x)),$$

where  $x$  is in the domain of definition of  $M$ . A period- $k$  point is defined as

$$P = M_k(P), \tag{10.3.18}$$

$$P \neq M_n(P) \quad \text{for all } n < k.$$

This means  $k$ -time mapped point  $P$  goes back to the starting point, and there is no sub-periodic point with period  $n < k$ .  $P$  is in the domain of  $M$ , and  $k$  and  $n$  are positive integers.

The Li-Yorke theorem is then as follows:  $M$  is a continuous map and has a domain over an interval  $J$ . If there is a point  $a$  in  $J$  for which the first iterate  $b = M(a)$ , the second iterate  $c = M(b)$ , and third iterate  $d = M(c)$  satisfy

$$d \leq a < b < c, \tag{10.3.19}$$

then the map has the following properties:

- There is an uncountable set  $S$  contained in  $J$  and containing no periodic points for which the following holds: for every  $p$  and  $q$  in  $S$  with  $p \neq q$

$$\lim_{n \rightarrow +\infty} \sup |M^n(p) - M^n(q)| > 0, \tag{10.3.20}$$

$$\lim_{n \rightarrow +\infty} \inf |M^n(p) - M^n(q)| = 0.$$

- For eve
- For eve

The first p eventually ke close intermi point. The unstable and

#### 10.3.2 Sat

##### 10.3.2.1 Co

The map to return map the upper ha trajectory st half  $x_2$  again chosen to re system. Jun  $x_1$ , while th the left side from the lo from the rig back to the may take pl

- The tr hits th  $2\pi/\omega$ .

In Fig this c

- The t it tur the u map, this c by

(10.2.16)

- For every positive integer  $k$  there is a periodic point in  $J$  of period  $k$ .
- For every  $p$  in  $S$  and every periodic point  $q$  in  $J$ ,

$$\lim_{n \rightarrow +\infty} \sup |M^n(p) - M^n(q)| > 0. \tag{10.3.21}$$

ie other, the parameters  
ion above, and knowing  
te the trajectories using

The first property is the chaos property. It states that any two chaotic points eventually keep wandering away from each other as well as coming arbitrarily close interminably. This property holds when  $M$  has  $d = a$ , a period-three point. The third property means that periodic points near chaotic ones are unstable and can turn into chaotic points under small perturbations.

**10.3.2 Satisfaction of the Li-Yorke theorem**

**10.3.2.1 Construction of the return map**

a first [5], then we will

. The maps are defined

(10.3.17)

t point is defined as

(10.3.18)

arting point, and there  
e domain of  $M$ , and  $k$

inuous map and has a  
which the first iterate  
e  $d = M(c)$  satisfy

(10.3.19)

containing no periodic  
id  $q$  in  $S$  with  $p \neq q$

(10.3.20)

The map to which we wish to apply the Li-Yorke theorem is the upper half axis return map [2]. Figure 10.2 shows a representation of the map. To construct the upper half axis return map,  $P_0$ , a point on the upper  $x_2$  axis is picked. The trajectory starting with this point is followed till it comes back to the upper half  $x_2$  again, and the  $x_2$  value of the return point is  $P_1$ .  $x_l = 0$ ,  $x_u = 0.3$  are chosen to restrict the interval  $J$  to be within 1. Notice that this is a two-state system. Jumping from one plane to the other is determined by the value of  $x_1$ , while this is a return map for  $x_2$ . When  $x_1$  exceeds the value of  $x_u$  from the left side and the state is on the lower plane originally, the trajectory jumps from the lower plane to the upper one. While when  $x_1$  gets smaller than  $x_l$  from the right side when the state is on the upper plane, the trajectory jumps back to the lower one. There are totally three possibilities that the trajectory may take place.

- The trajectory remains completely on the lower hysteresis plane when it hits the upper half  $x_2$  axis again. The time for a spiral to rotate  $360^\circ$  is  $2\pi/\omega$ . So in this case  $p_1$  is given by

$$p_1 = p_0 \exp(-2\sigma\pi/\omega). \tag{10.3.22}$$

In Fig. 10.2, the segment from point  $[0, 0]$  to  $[X_{sep}, X_{max}]$  corresponds to this case.

- The trajectory hits the  $x_u$  boundary and jumps to the upper plane before it turns back to the upper  $x_2$  axis. It needs to rotate another  $180^\circ$  to hit the upper  $x_2$  axis again after it jumps back to the lower plane. In the map, the segment from point  $[X_{sep}, X_{max}]$  to the point with  $P_1 = 0$  is for this case. The separation for the first case and the second case is given by

$$X_{sep} = x_u \exp((\sigma/\omega)(\pi + \arctan(\omega/\sigma))), \tag{10.3.23}$$

$$X_{max} = X_{sep} \exp(-2\sigma\pi/\omega). \tag{10.3.24}$$

- As in the second case, the trajectory jumps to the upper plane. When it jumps back to the lower plane it hits the upper  $x_2$  axis.

For the remaining two cases, the calculation of the mapping is rather more complicated than in the first case. No analytic formulas are available. Numerical results were obtained for these two cases. Combining these three cases together, the upper  $x_2$  return map is shown in Fig. 10.2.

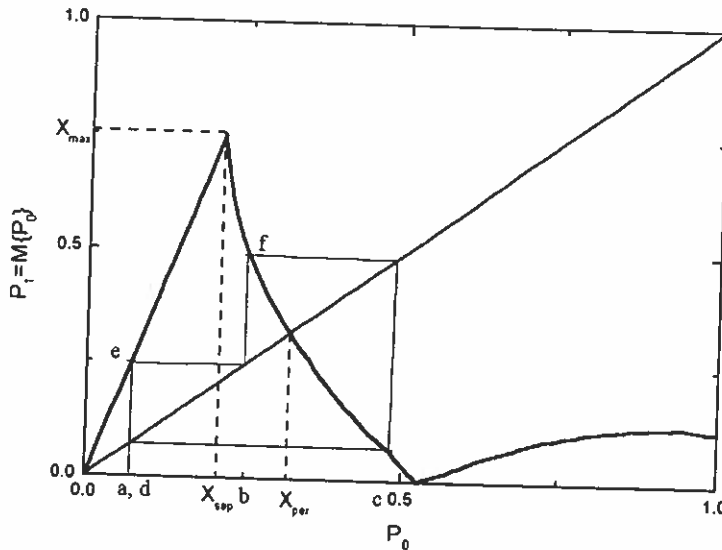


FIGURE 10.2  
 $x_2$  upper half axis return map [2].

### 10.3.2.2 Continuous condition for the return map

In fact the upper half-plane return map is generally not continuous as in Fig. 10.2, since there is a break at  $p_0 = X_{sep}$ . The condition for continuity of the upper half axis return map is that, the upper plane spiral  $T$  passes through point  $x_1 = x_u, x_2 = 0$ , and also passes through  $x_1 = 0, x_2 = b_0$ , as the lower plane spiral  $S$  does, shown in Fig. 10.3. By properly choosing design parameters  $a_2, \sigma$  to control the position of the upper plane spiral  $T$  and the shapes of both spirals, the continuity of the return map is guaranteed [2].

The design parameters for Eq. (10.2.7) are shown in equation (10.3.25).

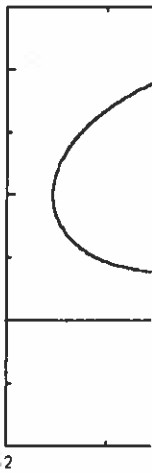


FIGURE 10.3  
Continuity of binary state

### 10.3.2.3 Period three po

In order to have chaotic period-three point.

The horizontal axis  $P_0$  slope line in the diagram to  $d$  in the figure, so they point  $e$ . The  $P_1$  value of symmetry to the unit slope indicates the value  $c$  on the starting point  $a$ .

In fact, the period three



(10.3.24)

ane. When it

s rather more available. Nu- se three cases

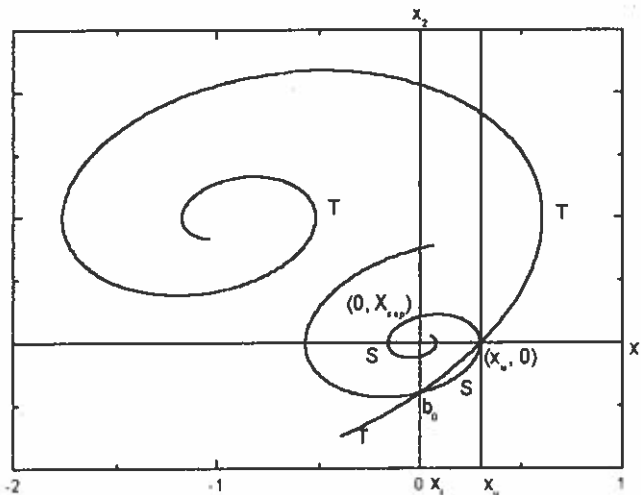


FIGURE 10.3 Continuity of binary state system [2].

$$\begin{aligned}
 a_1 &= -1, & a_2 &= -1.35, \\
 \sigma &= -0.2, \\
 x_l &= 0, & x_u &= 0.3, \\
 h_+ &= 1, & h_- &= 0.
 \end{aligned}
 \tag{10.3.25}$$

10.3.2.3 Period three points

In order to have chaotic properties, the map should be continuous and have a period-three point.

The horizontal axis  $P_0$  in Fig. 10.2 is for  $x_2$ . As a visual aid we put a unit slope line in the diagram. Points  $a, b, c$  and  $d$  satisfy Eq. (10.3.19).  $a$  is equal to  $d$  in the figure, so they are period-three points. From  $a$ , we get the mapped point  $e$ . The  $P_1$  value of point  $e$  is the  $P_0$  value of the next turn, which, by symmetry to the unit slope line, is  $b$ . The mapped point for  $b$  is point  $f$ , which indicates the value  $c$  on  $P_0$  for the next turn. Finally the trace goes back to the starting point  $a$ .

In fact, the period three point condition for chaotic properties do not effect

us as in Fig. inuity of the sses through =  $b_0$ , as the osing design d  $T$  and the teed [2]. 10.3.25).

our designing parameters, as long as it is satisfied.

### 10.4 Binary Hysteresis Design

#### 10.4.1 Semistate description of hysteresis

The function given in Eq. (10.2.2) is called binary hysteresis. Figure 10.4 shows a typical example of binary hysteresis. The curve can be described by

$$y = \begin{cases} H_+ & \text{for } \begin{cases} u_+ < u \text{ or} \\ u_- \leq u \leq u_+ \text{ if } y_0 = H_+, \end{cases} \\ H_- & \text{for } \begin{cases} u_- \leq u \leq u_+ \text{ if } y_0 = H_- \text{ or} \\ u < u_-, \end{cases} \end{cases} \quad (10.4.26)$$

where  $H_+$  and  $H_-$  are the values of  $y$  for the upper state and lower state respectively.  $u_+$  and  $u_-$  are two boundaries. Here, we assume

$$H_- < H_+, \quad u_- \leq u_+, \quad (10.4.27)$$

$y_0$  is the previous value of  $y$ .

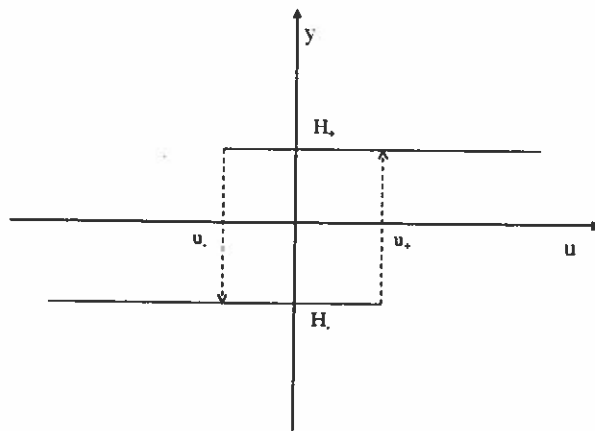


FIGURE 10.4 Binary hysteresis.

For the purpose of implementation, we use a different mathematical repre-

sensation. It g

where  $f(\cdot)$  is a parameters:

$$a = \overline{f}$$

$$z_a = 1$$

The first eq for the line a decided by  $z_a$ .

To check th we let the line to  $+\infty$ . The r again, which i

FIGURE 10.5 Creation of b

#### 10.4.2 Hy

With the ser can be realiz

sensation. It gives the same hysteresis as Eq. (10.4.27) does.

$$y = (1 + \frac{1}{a})z - \frac{1}{a}u, \tag{10.4.28}$$

$$y = f(z - z_a).$$

where  $f(\cdot)$  is a step function,  $a$  and  $z_a$  are constants which depend on hysteresis parameters:

$$a = \frac{(u_+ - u_-)}{(H_+ - H_-) - (u_+ - u_-)}, \tag{10.4.29}$$

$$z_a = u_+ + \frac{a}{1+a}H_- = \frac{1}{2}[(u_+ + u_-) + \frac{a}{1+a}(H_+ + H_-)].$$

The first equation is a straight line for  $y$  vs.  $z$ . Figure 10.5 shows the graph for the line and step function. The position for the step function, which is decided by  $z_a$ , is fixed, while the line is not because  $u$  is arbitrary.

To check that the semistate equations give a binary hysteresis as in Fig. 10.4, we let the line sweep from the left to right by changing the value of  $u$  from  $-\infty$  to  $+\infty$ . The number of intersections changes from one to two and then to one again, which is the same as  $y$  in Fig. 10.4.

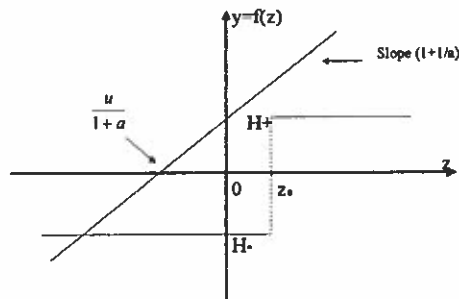


FIGURE 10.5  
Creation of binary hysteresis via semistate equations [6].

### 10.4.2 Hysteresis description for circuit

With the semistate description in mind, we can go on to the description that can be realized by a circuit. Because we are using current based circuit, the

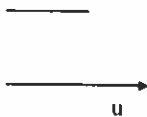
hysteresis. Figure 10.4 shows  
can be described by

$$z_+, \tag{10.4.26}$$

or

upper state and lower state  
we assume

$$\tag{10.4.27}$$



different mathematical repre-

input for hysteresis is voltage and the output is current. In other words, we take  $V_{in}$  as the horizontal axis  $z$ , and  $I_o$  as the vertical axis  $y$ . The original equations for our circuits are of the form (realization of equations using a circuit will be fully discussed in the following sections):

$$\begin{aligned} V_1 + V_2 &= V_{in}, \\ I_o &= f(V_{in} - V_a), \\ I_o &= K \times V_2. \end{aligned} \quad (10.4.30)$$

Here,  $f(\cdot)$  is, again, a step function.  $V_a$  is a constant which controls the position of the step function.  $K$  is the slope of the sweep line.  $V_1$  and  $V_2$  are dependent variables. Transforming the Eq. (10.4.30) into the format of Eq. (10.4.28) gives the relationships between  $I_o$  and  $V_{in}$ :

$$\begin{aligned} I_o &= KV_{in} - KV_2, \\ I_o &= f(V_{in} - \frac{I_o}{K} - V_a). \end{aligned} \quad (10.4.31)$$

By comparing this set of equations to Eq. (10.4.28), we can see  $I_o$  vs.  $V_{in}$  is like  $y$  vs.  $z$ , and  $V_2$  is like  $u$ . From Eq. (10.4.30), we have:

$$V_2 = V_{in} - V_1 = V_{in} - \frac{I_o}{K}. \quad (10.4.32)$$

$I_o$  is somewhat like a constant, taking only two values, which are decided by the state of the step function. The range of  $V_{in}$  is not defined, so  $V_2$  can be any value. Therefore the line decided by Eq. (10.4.32) can sweep over the  $x$ -axis intrinsically.

The second equation of (10.4.30) is, by itself, a binary hysteresis. When  $I_o$  takes the high value,  $I_+$ , and when  $V_{in}$  is high originally, the location of the right half of the step function is  $I_+/K + V_a$ . If  $I_o$  takes the low value,  $I_-$ , and when  $V_{in}$  is low, the location of the left half of the step function is  $I_-/K + V_a$ .

#### 10.4.3 Design parameters for hysteresis generation

To generate chaos, the width, the height, as well as the location of hysteresis need to be chosen carefully. In this section we discuss mathematically the design parameters.

Because of the restriction on the characteristics of transistors and circuit properties, the actual step function can not be as steep as in Fig. 10.5. There is a transient band between the high branch and the low branch, as is shown in Fig. 10.6. In the figure,  $x_l$  and  $x_u$ , two boundaries of hysteresis, are the

intersections of the corner points of the see, it is not so in are, and neither t other simpler ways is the width of hyst parameters.

FIGURE 10.6 Unideal step funct

The factors tha the step function t of the sweep line.

Using the formula width:

If, unfortunately, function, which is will consequently sweep line, which the high frequency

Theoretically, tl tion. But, in prac

n other words, we is  $y$ . The original ions using a circuit

$$(10.4.30)$$

ontrols the position  $V_2$  are dependent Eq. (10.4.28) gives

$$(10.4.31)$$

see  $I_o$  vs.  $V_{in}$  is

$$(10.4.32)$$

h are decided by so  $V_2$  can be any p over the  $x$ -axis

teresis. When  $I_o$  e location of the ow value,  $I_-$ , and on is  $I_-/K + V_a$ .

tion of hysteresis thematically the

stors and circuit Fig. 10.5. There nch, as is shown /steresis, are the

intersections of horizontal axis with sweep lines when they go through the corner points of the step function. In the later sections of the chapter we will see, it is not so important what the high value  $H_+$  and the low value  $H_-$  are, and neither the  $x_l$  and  $x_u$  of the hysteresis. They can be adjusted by other simpler ways rather than changing device sizes. What is really critical is the width of hysteresis, i.e.,  $x_u - x_l$ , which must be decided by the circuit parameters.

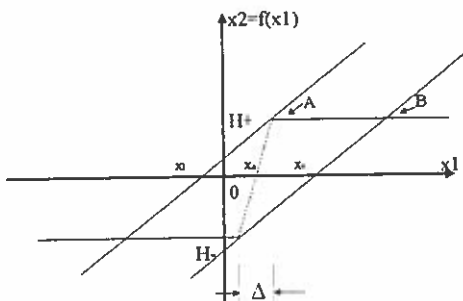


FIGURE 10.6 Unideal step function and sweep hysteresis.

The factors that effect the width are, seen from Fig. 10.6,  $\Delta$ , the width of the step function transient area,  $h$ , the height of the step function,  $k$  the slope of the sweep line. From the figure, we notice:

$$x_u - x_l = \text{interval } A - B. \tag{10.4.33}$$

Using the formulas for triangles, we can finally come with the equation for the width:

$$x_u - x_l = \frac{h}{K} - \Delta. \tag{10.4.34}$$

If, unfortunately,  $\Delta$  is large, we shall have to increase the height of the step function, which is restricted by the circuit voltage source  $V_{dd}$  and  $V_{ss}$  and will consequently increase the power consumption, or decrease the slope of the sweep line, which will reduce the sharpness of the hysteresis and so will effect the high frequency performance, i.e. when vibration of chaos speeds up.

Theoretically, the width of the hysteresis can be anything before normalization. But, in practice, wider hysteresis width implies wider operation range of

$X_1$  and  $X_2$ , which challenge the linear operation range of the differential pairs. In the circuit design, 0.3 V to 0.4 V was used as a guide line for the width of the hysteresis.

### 10.5 VLSI Realization of Current Based Degree-Two Chaos Generator

In this section, a current based degree-two chaos generator is described in detail.

#### 10.5.1 Block diagram and system equations

The block diagram of the current based chaos circuit is shown in Fig. 10.7. Here, capacitors are used to realize the derivative.  $G_1$ ,  $G_2$ , and  $G_6$  are linear transconductance functions with different transconductances,  $gm$ : which turn capacitor voltages into currents. The hysteresis part is surrounded by the dash box in Fig. 10.7 which is primarily due to [3].  $G_3$  is a step function OTA (operational transconductance amplifier), while  $G_4$  is a linear transconductor of transconductance  $gm_4$ , and serves to give a resistive sweep line on the characteristics of  $G_3$  as discussed in Sec. 1.4.2. The multiple output currents of  $G_3$  and  $G_4$  have the shape of hysteresis with width fixed by  $gm_4$ .  $F_1$  and  $F_2$  are current mirror with different gain which also control the output current levels to adjust the vertical positions of the hysteresis.

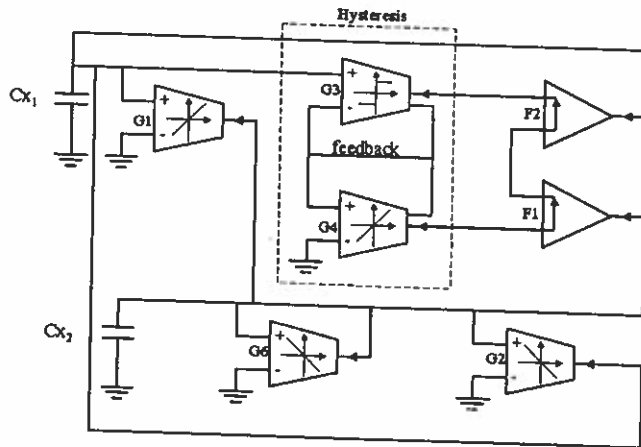


FIGURE 10.7 Ideal component circuit of chaos generation system.

### VLSI Realization

To avoid conf output end of e can be written : the correspondi width  $X_U$ , with

For simplicity with Eq. (10.5.:

To normalize has to be satisf

Equations (1 eters of  $gm_1$ ,  $g$  Differential p for the circuit,

#### 10.5.2 Tran 10.5.2.1 Com

Figure 10.8 shc from the Fig. used to implen Differential ; tions. The ste block.  $G_1$ ,  $G_2$   $F_1$  and  $F_2$  are

To avoid confusion, all the current directions are marked with arrows at the output end of each building block in Fig. 10.7. Thus, the system equations can be written as Eq. (10.5.35).  $gm_1$ ,  $gm_2$ , and  $gm_6$  are transconductances of the corresponding OTA.  $H(V_1)$  is the hysteresis function with height  $H_+$  and width  $X_U$ , with  $H_-$  and  $X_L$  are adjusted to zero.

$$\begin{aligned}
 C_{x1} \frac{dV_1}{dt} &= -gm_2 V_2 - F_2 H(V_1), \\
 C_{x2} \frac{dV_2}{dt} &= -gm_1 V_1 - gm_6 V_2 - F_1 H(V_1), \\
 H(V_1) &= \begin{cases} H_+ & \text{if } X_L = 0 < V_1, \\ 0 & \text{if } V_1 < X_U. \end{cases}
 \end{aligned}
 \tag{10.5.35}$$

For simplicity,  $C_{x1}$  and  $C_{x2}$  are chosen to be equal. By comparing Eq. (10.2.1) with Eq. (10.5.35), Eq. (10.5.36) is obtained.

$$\frac{-gm_2}{1} = \frac{-F_2}{a_1} = \frac{-gm_1}{-1} = \frac{-gm_6}{-2\sigma} = \frac{-F_1}{a_2}.
 \tag{10.5.36}$$

To normalize Eq. (10.5.35) to Eq. (10.2.7), another proportional relationship has to be satisfied, as shown in Eq. (10.5.37).

$$\frac{H_+}{X_U} = \frac{1}{x_u}.
 \tag{10.5.37}$$

Equations (10.5.36) and (10.5.37) are used later to decide the design parameters of  $gm_1$ ,  $gm_2$ , and  $gm_6$ .

Differential pairs are used to implement all the linear and step function OTA for the circuit, which will be discussed in detail in the next section.

### 10.5.2 Transistor implementation

#### 10.5.2.1 Complete transistor level current based chaos generator

Figure 10.8 shows the the complete current based chaos generator as translated from the Fig. 10.7 to transistor circuit. AMI 1.2  $\mu m$  technology models are used to implement the circuit.  $V_{dd}$  and  $V_{ss}$  are biased to  $V_{dd} = -V_{ss} = 5 V$ .

Differential pairs are important building blocks to give step or linear functions. The step function  $G3$  and the linear function  $G4$  form the hysteresis block.  $G1$ ,  $G2$ , and  $G4$  are linear functions with different transconductances.  $F1$  and  $F2$  are current mirrors with different gains.

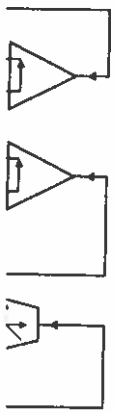
ee-Two Chaos Generator

of the differential pairs. The line for the width of

ree-Two Chaos

or is described in detail.

is shown in Fig. 10.7.  $G2$ , and  $G6$  are linear functions,  $gm$ : which turn surrounded by the dash a step function OTA linear transconductor weep line on the char-output currents of  $G3$   $gm_4$ .  $F1$  and  $F2$  are output current levels



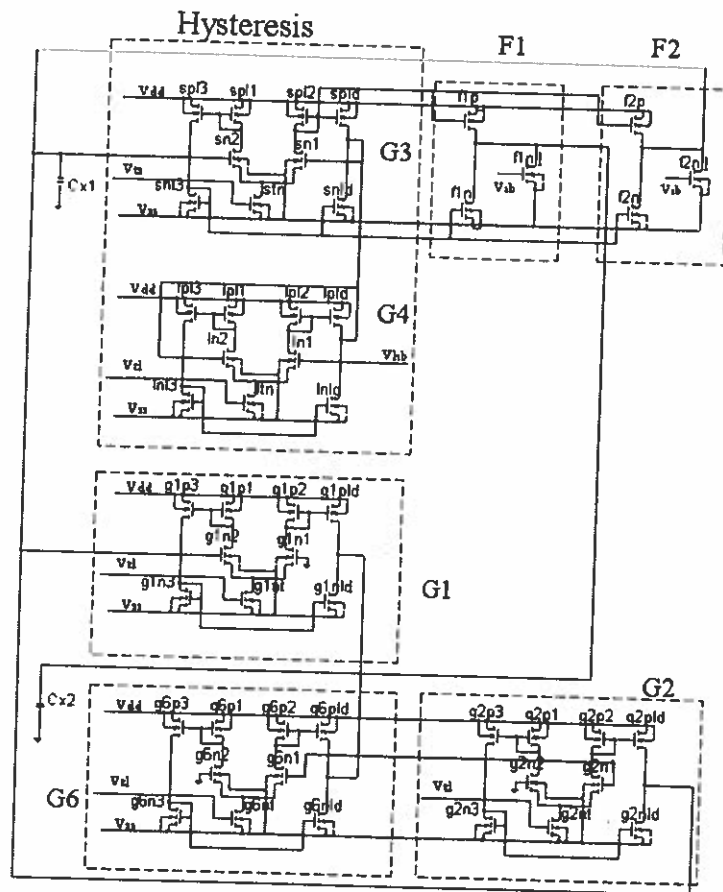


FIGURE 10.8 Transistor circuit for hysteresis generation.

10.5.2.2 Implementatio pairs

As we mentioned earlier tial pairs. Figure 10.9 is *Mndp1* and *Mndp2* are rent sink transistor *Mn* *Mndp1* and *Mndp2* is c are transmitted to the is the difference between and *Mndp2*. As we can gives current as the out

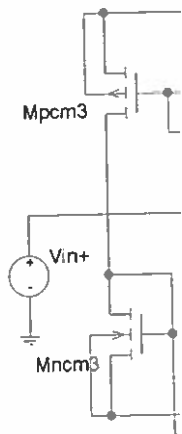


FIGURE 10.9 Differential pair used i

By increasing the  $v$  transistor *Mnt* to inc region can be increase and *Mndp2*, the slop region is narrow enou the transient region is as a linear function. voltage, we can imple same circuit structur but a general guideli work independently.



### 10.5.2.2 Implementation of linear and step functions through differential pairs

As we mentioned earlier, the linear and step functions are realized by differential pairs. Figure 10.9 is the differential pair that we use throughout the system. *Mndp1* and *Mndp2* are the input stage, whose current is provided by the current sink transistor *Mnt*. The current distribution in the two input transistors *Mndp1* and *Mndp2* is controlled by their gate voltages, and these two currents are transmitted to the output stage by current mirrors. The output current is the difference between the two currents passing through transistors *Mndp1* and *Mndp2*. As we can see, this differential pair takes voltage as the input and gives current as the output.

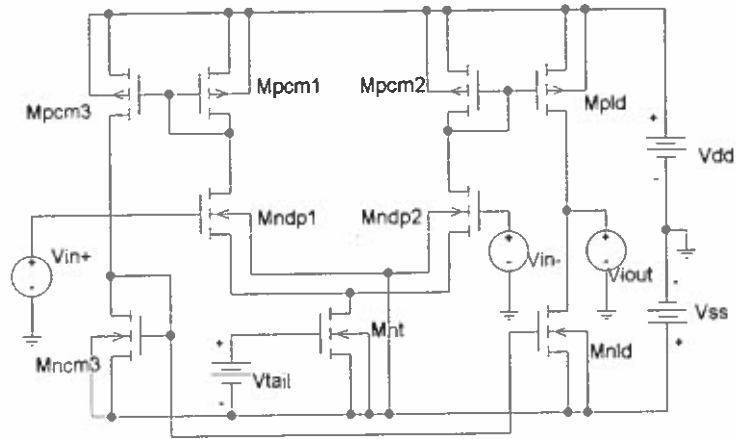
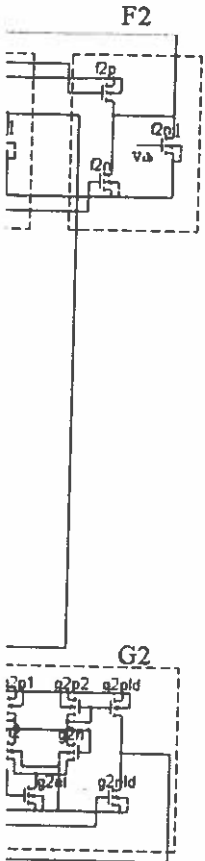


**FIGURE 10.9**  
Differential pair used in our circuit.

By increasing the width to length ratio and gate voltage  $V_{tail}$  of the tail transistor *Mnt* to increase the current sinking down through *Mnt*, the linear region can be increased. By varying the parameters of the transistors *Mndp1* and *Mndp2*, the slope of the linear region can be adjusted. When the linear region is narrow enough, the output curve can be used as a step function. If the transient region is wide and straight enough, the output curve can be used as a linear function. In other words, by adjusting device parameters and bias voltage, we can implement either step functions or linear functions using the same circuit structure, the differential pair. This is not an exact description but a general guideline of how to adjust the circuit, since none of the factors work independently.

In Fig. 10.10, an example of the linear and step functions is given. The  $I_{step}$  curve is a step function generated by a differential pair, which is used as  $G3$ . The  $I_{linear}$  curve is the linear function in the region between  $-0.6 V$  and  $0.6 V$ , which is used as  $G4$ .

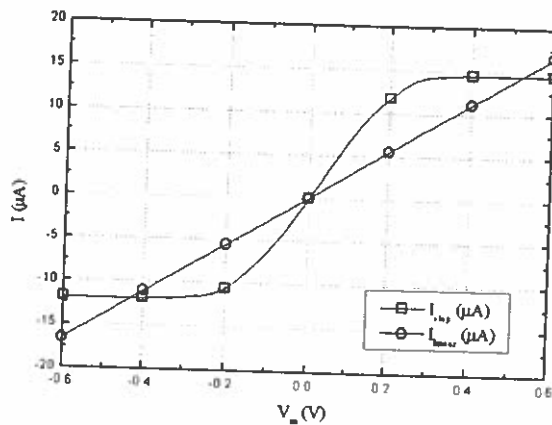


FIGURE 10.10 An example of the step and linear functions of output current vs. input voltage.

10.5.2.3 Realization of hysteresis

As shown in Fig. 10.8, the hysteresis part is generated by a step function  $G3$  and a linear function  $G4$ . At this stage,  $X_L$  is adjusted to  $0 V$  by biasing the gate voltage of transistor  $ln1$ . The current mirror  $F2$  is formed by a pair of transistors  $f2p$  and  $f2n$ , which mirror the currents of transistors  $spld$  and  $snld$  in  $G3$ . The difference between the two currents of  $f2p$  and  $f2n$  is shifted by a constant current source  $f2nl$  to adjust the lower value of the hysteresis to be zero. The hysteresis output current of  $F1$  with  $X_L = 0$  and  $H_L = 0$  is then supplied to the capacitor  $C_{x1}$ . Current mirror  $F1$  works in a similar way as  $F2$ , except the proportional variation of the transistors' sizes. To satisfy the proportional relationship shown in Eq. (10.5.36), the hysteresis current output of  $F1$  has the same width but  $a_2/a_1 = 1.35$  times the height of the output of  $F2$ . This current is fed to capacitor  $C_{x2}$ . The output currents of the hysteresis block,  $F1$ , and  $F2$  are shown in Fig. 10.11.

As shown in Fig. 10.11, the two switching points for the hysteresis curves occur at  $X_L = 0 V$  and  $X_U = 0.373 V$ . In order to normalize  $X_U$  to  $x_u = 0.3$ , with Eq. (10.5.37),  $H_+$  must take the value  $1.243 V$ . The top value of the

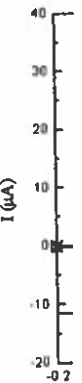


FIGURE 10.11 One example of binary hysteresis block.  $I_{F2}$  the output currents c

hysteresis output of  $I$  as can  $F_2$ , as shown

10.5.2.4 Complete

With the knowledge  $G2$ , and  $G2$  can be c and the chaotic con can be decided.

All the transistor ble 10.1. The bias p

For all the linear f are biased to a tail the sink transistor s of transistors  $f1nl$  ε which is also the ga

$$gm_1 =$$

With the transist

s is given. The  $I_{step}$  which is used as  $G3$ .  $n - 0.6 V$  and  $0.6 V$ ,

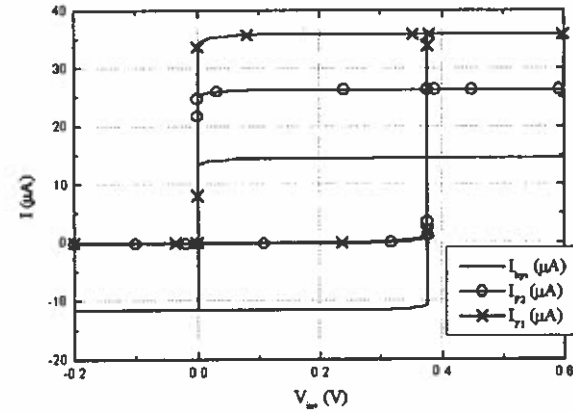


**FIGURE 10.11**  
One example of binary hysteresis.  $I_{hys}$  (solid line) is the output current of the hysteresis block.  $I_{F2}$  (solid line with circle) and  $I_{F1}$  (solid line with cross) are the output currents of  $F2$  and  $F1$ .

it vs. input voltage.

hysteresis output of  $F_1$  is  $F_1 H_+ = 26.30 \mu A$ . The value of  $F_1$  can be calculated, as can  $F_2$ , as shown in Eq. (10.5.38).

$$F_1 = 21.15 \frac{\mu A}{V}, \quad F_2 = 28.88 \frac{\mu A}{V}. \quad (10.5.38)$$

a step function  $G3$   $0 V$  by biasing the formed by a pair of sources  $spld$  and  $snld$   $f2n$  is shifted by the hysteresis to be and  $H_L = 0$  is then in a similar way as ses. To satisfy the esis current output it of the output of ts of the hysteresis

10.5.2.4 Complete circuit parameters and bias voltages

With the knowledge of the two hysteresis outputs, the transconductances of  $G1$ ,  $G2$ , and  $G2$  can be decided accordingly. The calculation involves Eq. (10.5.36) and the chaotic conditions in Eq. (10.3.25). Thus, all the design parameters can be decided.

All the transistor sizes of the chaos generator in Fig. 10.8 are listed in Table 10.1. The bias points voltages are listed in Table 10.2.

For all the linear functions, the gate voltages of all the current sink transistors are biased to a tail voltage  $V_{tl}$ . For the step function  $G3$ , the gate voltage of the sink transistor  $stn$  is biased to another tail voltage  $V_{ts}$ . The gate voltages of transistors  $f1nl$  and  $f2nl$  are biased to  $V_{ib}$ . The negative input end of  $G4$ , which is also the gate voltage of transistor  $ln1$ , is biased to  $V_{hb}$ .

$$gm_1 = -gm_2 = 21.13 \frac{\mu A}{V}, \quad gm_6 = 8.33 \frac{\mu A}{V}. \quad (10.5.39)$$

hysteresis curves the  $X_U$  to  $x_u = 0.3$ , e top value of the

With the transistor parameters in Table 10.1 and the bias point informa-

Part Name	Parameter	Part Name	Parameter	Part Name	Parameter
g1p1	15.2:4	g1p2	15.2:4	g1p3	4:4
g1p1d	30.4:36	g1nt	24:4	g1n3	4:4
g1n1d	28.8:36:4	g1n1	4:4	g1n2	4:4
g2p1	15.2:4	g2p2	15.2:4	g2p3	4:4
g2p1d	30.4:36	g2nt	24:4	g2n3	4:4
g2n1d	28.8:36:4	g2n1	4:4	g2n2	4:4
g6p1	44:4	g6p2	44.8:4	g6p3	4:4
g6p1d	16:16	g6nt	24:4	g6n3	4:4
g6n1d	16:16.8	g6n1	4:4	g6n2	4:4
sp11	4:4	sp12	4:4	sp13	24:4
sp1d	24:4	stn	12:4	sn13	8:4
sn1d	8:4	sn1	4:4	sn2	4:4
lp11	12:4	lp12	12:4	lp13	4:4
lp1d	4:4	ltn	24:4	ln13	4:4
ln1d	4:4	ln1	4:4	ln2	4:4
f1p	32:4	f1n	10.4:4	f1n1	9.6:8
f2p	24:4	f2n	8:4	f2n1	4:4

TABLE 10.1  
Design parameters for transistors ( $W(\mu m) : L(\mu m)$ ).

tion in Table 10.2, the transconductances of  $G_1$ ,  $G_2$ , and  $G_6$  are given in Eq. (10.5.39). Then the system Eqs. (10.5.35) can be written as Eqs. (10.5.40).

$$\begin{aligned}
 C_{x1} \frac{dV_1}{dt} &= 21.13 \frac{\mu A}{V} \times V_2 - 26.30 \mu A \times h(V_1), \\
 C_{x2} \frac{dV_2}{dt} &= -21.13 \frac{\mu A}{V} \times V_1 + 8.33 \frac{\mu A}{V} \times V_2 - 35.90 \mu A \times h(V_1), \\
 h(V_1) &= \begin{cases} 1 & \text{if } X_L = 0V < V_1, \\ 0 & \text{if } V_1 < X_U = 0.373V. \end{cases}
 \end{aligned}
 \tag{10.5.40}$$

Equation (10.5.40) can be normalized to Eq. (10.2.7) and satisfies the chaotic parameter conditions in Eq. (10.3.25).

The exact values of the two capacitors are not crucial, although they are chosen to be equal, since they only effect the time scale. However, the value of the capacitors can not shrink indefinitely, because they must swamp the parasitics of the hysteresis and thus the circuit would not function when the capacitance is too small. In our simulations, when the capacitances are smaller than the order of nanofarads, the circuit was no longer chaotic. The simulation results shown in the next section were obtained when  $C_{x1} = C_{x2} = 21 \text{ nF}$ .

Bias point	Bias voltage
$V_{dd}$	5
$V_{ts}$	-
$V_{hb}$	0

TABLE 10.2  
Bias point voltages.

### 10.6 Discussion

Chaotic signals are is modified even slight it does not change  $[0, 0]$  if possible, since so far presented, [C means of transform

The reason why because it is the equilibrium point of the lower plane can be set at be achieved by shift becomes Eq. (10.6.

The two equilibrium  
Lower plane:

upper plane:

The transistor in is based on the circuit two current source

### 10.7 Simulation

The theory was checked simulations were in 1.2  $\mu m$  transistor ; Figure 10.12 shows zero initial condition

Parameter
4:4
4:4
4:4
4:4
4:4
4:4
4:4
4:4
24:4
8:4
4:4
4:4
4:4
4:4
9.6:8
4:4

Bias point	Bias value (V)	Bias point	Bias value (V)
$V_{dd}$	5.0	$V_{ss}$	-5.0
$V_{ts}$	-4.4	$V_{it}$	-3.0
$V_{hb}$	0.38	$V_{ib}$	-3.73

TABLE 10.2  
Bias point voltages.

### 10.6 Discussions on Initial Conditions

Chaotic signals are extremely sensitive to initial conditions. If the initial value is modified even slightly, its signal will be totally different later, even though it does not change the signal's chaotic properties. Thus it is preferable to use  $[0, 0]$  if possible, since the origin is a reliably set point. However, in the system so far presented,  $[0, 0]$  is not a convenient initial point, so here we discuss a means of transforming the system such that  $[0, 0]$  is a convenient initial point.

The reason why  $[0, 0]$  point should not be chosen as the initial condition is because it is the equilibrium point of the lower plane spiral. If the equilibrium point of the lower plane spiral can be moved away from  $[0, 0]$ , then the initial point can be set at  $[0, 0]$ , which makes the system a lot easier to run. This can be achieved by shifting the  $X_2$  coordinate with a constant  $s$ . Then, Eq. (10.2.7) becomes Eq. (10.6.41):

$$\begin{aligned} \frac{dx_1}{dt} &= (x_2 - s) + a_1 h(x_1) \\ \frac{dx_2}{dt} &= -x_1 - 2\sigma(x_2 - s) + a_2 h(x_1) \end{aligned} \tag{10.6.41}$$

The two equilibrium points in this figure are moved to:  
*Lower plane:*

$$[x_1, x_2] = [0, s] \tag{10.6.42}$$

*upper plane:*

$$[x_1, x_2] = [2\sigma a_1 + a_2, -a_1 + s] \tag{10.6.43}$$

The transistor implementation of this non-equilibrium system for Eq. (10.6.41) is based on the circuit for the original system, and modified by simply adding two current sources to the existing circuit, one for each capacitor.

### 10.7 Simulation Results

The theory was checked via PSpice computer simulations. The results for these simulations were in agreement with the theory. In PSPICE simulations, MOSIS 1.2  $\mu\text{m}$  transistor models were used (AMI 1.2 $\mu\text{m}$  run N7AB).

Figure 10.12 shows the trajectory in the  $X_1 - X_2$  plane. It is for a non-zero initial condition system. We can see from the figure that the center of

'6 are given in  
Eqs. (10.5.40).

),  
(10.5.40)

id satisfies the  
ough they are  
ever, the value  
ust swamp the  
ction when the  
ices are smaller  
The simulation  
 $\epsilon_2 = 21 \text{ nF}$ .

the bottom spiral is located on the original point. The spirals switch to the trajectories up and down as it hits the hysteresis edges at  $X_L$  and  $X_U$ . The trajectory fills up a region of the plane, indicating the possible presence of chaotic behavior.

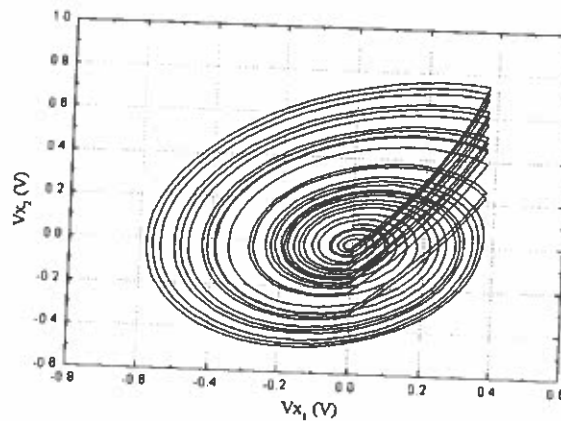


**FIGURE 10.12**  
Phase plane trajectory for a non-zero initial condition system.  
 $V_{x1} = V_1, V_{x2} = V_2$ .

Figure 10.13 and Fig. 10.14 are the simulation results for a zero initial condition system. As shown in Fig. 10.13, the equilibrium point of this system is moved downwards to  $V_{x2} = -0.2V$ , compared with Fig. 10.12. The chaotic signal  $V_{x2}$  varying with time is shown in Fig. 10.14. The signal starts from  $V_{x2} = 0$  at  $time = 0$ , indicating that its initial value can be zero.

### 10.8 Conclusions

In this chapter we have presented a current based chaos generation system. This system is based on the Li-Yorke theorem, and using binary hysteresis, the current based model that we used and the mathematical model for hysteresis generation enabled us to implement the system with great simplicity. A scheme is proposed to change the initial points of the system, so that we are able to save rather elaborate hardware necessary to set the initial values of the two capacitors. Also, the simulations that have been carried out demonstrated the validity of our model.

**FIGURE 10**  
Phase plane

**FIGURE 10**  
Chaotic sign  
 $C_{x2}$  were 21

The spirals switch to the  
ages at  $X_L$  and  $X_U$ . The  
the possible presence of



system.

Its for a zero initial con-  
cum point of this system  
Fig. 10.12. The chaotic  
The signal starts from  
an be zero.

chaos generation system.  
ng binary hysteresis. the  
ical model for hysteresis  
eat simplicity. A scheme  
t, so that we are able to  
initial values of the two  
ed out demonstrated the

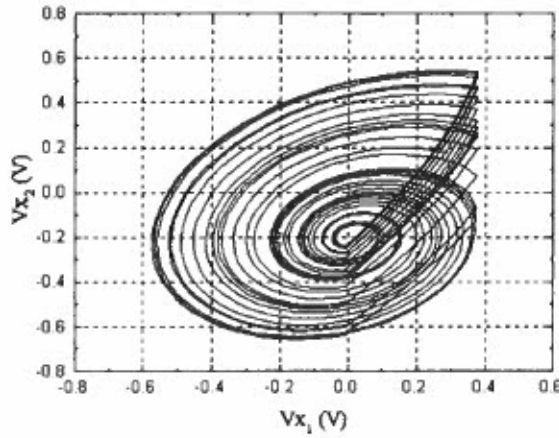


FIGURE 10.13  
Phase plane trajectory for a zero initial condition system.  $V_{x1} = V_1, V_{x2} = V_2$ .

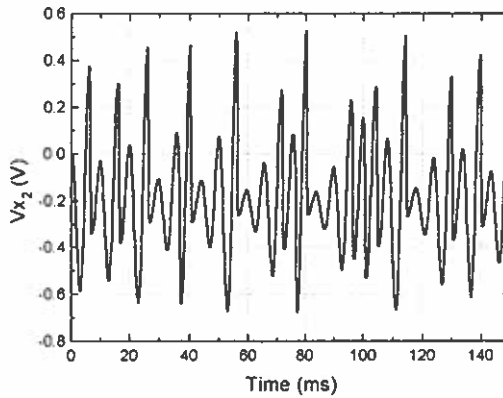


FIGURE 10.14  
Chaotic signal  $V_{x2} = V_2$  vs. time when the two simulating capacitors  $C_{x1}$  and  $C_{x2}$  were 21 nF.

## References

- [1] O. E. RöSSLer, "Continuous chaos-four prototype equations," *Bifurcation Theory and Applications in Scientific Disciplines*, Vol. 316, pp. 316, 1979.
- [2] R. W. Newcomb and N. El-Leithy, "Chaos generation using binary hysteresis," *Circuit Systems Signal Process*, Vol. 5, No. 3, pp. 321-341, 1986.
- [3] S. Nakagawa and T. Saito, "CMOS hysteresis chaos generator with ISS control," *IEEE/ISCAS*, Hong Kong, pp. 797-800, June 9-12, 1997.
- [4] J. E. Varrientos and E. Sanchez-Sinencio, "A 4-D chaotic oscillator based on a differential hysteresis comparator," *IEEE Trans. CAS-I*, Vol. 45, No. 1, pp. 3-10, 1998.
- [5] T.-Y. Li and J. A. Yorke, "Period three implies chaos," *Amer. Math. Monthly*, Vol. 82, pp. 985-992, 1975.
- [6] R. W. Newcomb, "Semistate design theory binary and swept hysteresis," *Circuits Systems Signal Process*, Vol. 1, No. 2, pp. 204-216, 1982.

## 11

## Stochastic

Michaël Antonie

<sup>1</sup> Department of  
Rand Afrikaans U  
mavw@ing1.rau.za

<sup>2</sup> Department of  
The University of  
Jiu.Ding@usm.ed

## Abstract

In this cha  
erators, th  
namical sy  
results on  
the direct  
of the fixe  
measure u  
theory an  
electrical c



WORLD SCIENTIFIC SERIES ON  
**NONLINEAR SCIENCE**

Series B Vol. 11

Series Editor: Leon O. Chua

# CHAOS IN CIRCUITS AND SYSTEMS

edited by

**Guanrong Chen**  
City University of Hong Kong, China

**Tetsushi Ueta**  
Tokushima University, Japan

 **World Scientific**  
New Jersey • London • Singapore • Hong Kong

2002